

10.1071/CH20074_AC

©CSIRO 2021

Australian Journal of Chemistry 2021, 74(2), 145-150

Supplementary Material

Chiral BINAPO Induced Circularly Polarized Luminescence in a Triple-Stranded Eu₂L₃(BINAPO)₂ Helicate

Shuang Bi,^A Yanyan Zhou,^A Yuan Yao,^A Zhenyu Cheng,^A Ting Gao,^{A,B} Pengfei Yan,^A and Hongfeng Li^{A,B}

^AKey Laboratory of Functional Inorganic Material Chemistry (Ministry of Education), School of Chemistry and Materials Science, Heilongjiang University, No. 74, Xuefu Road, Nangang District, Harbin 150080, China.

^BCorresponding authors. Email: gaotingmail@sina.cn; lihongfeng@hlju.edu.cn

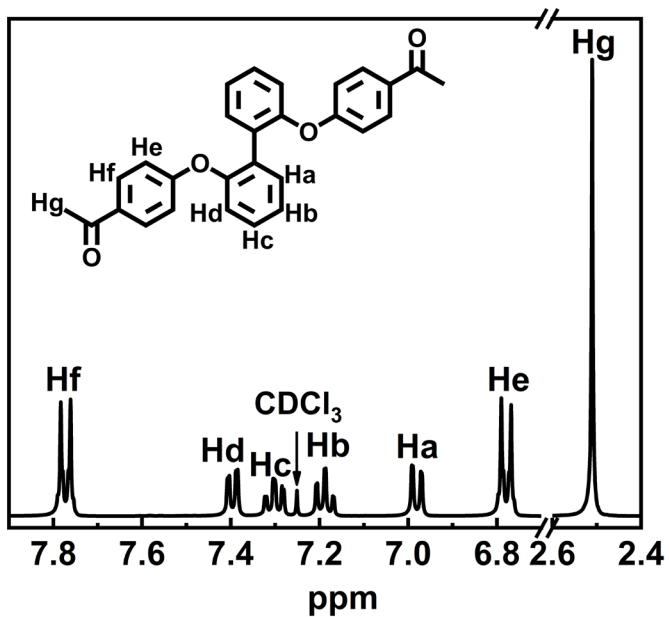


Fig. S1. 400 MHz ^1H NMR spectrum of 4,4'bin-(acetyl)phenoxy-1,1'-biphenyl in CDCl_3 .

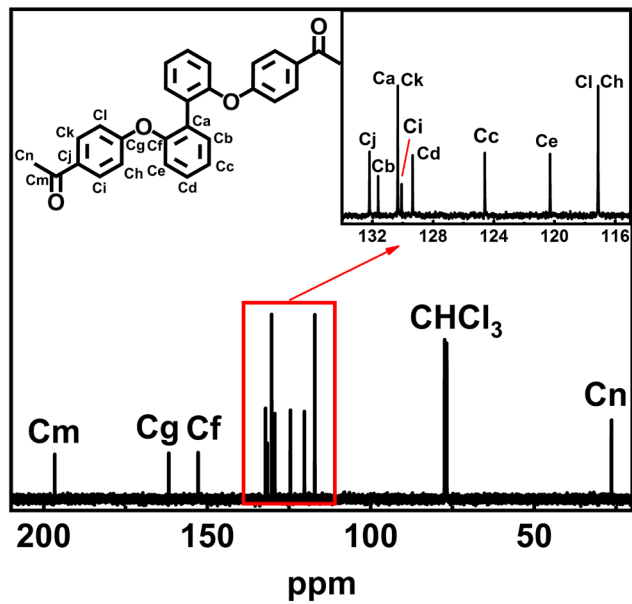


Fig. S2. 101 MHz ^{13}C NMR spectrum of 4,4'bin-(acetyl)phenoxy-1,1'-biphenyl in CDCl_3 .

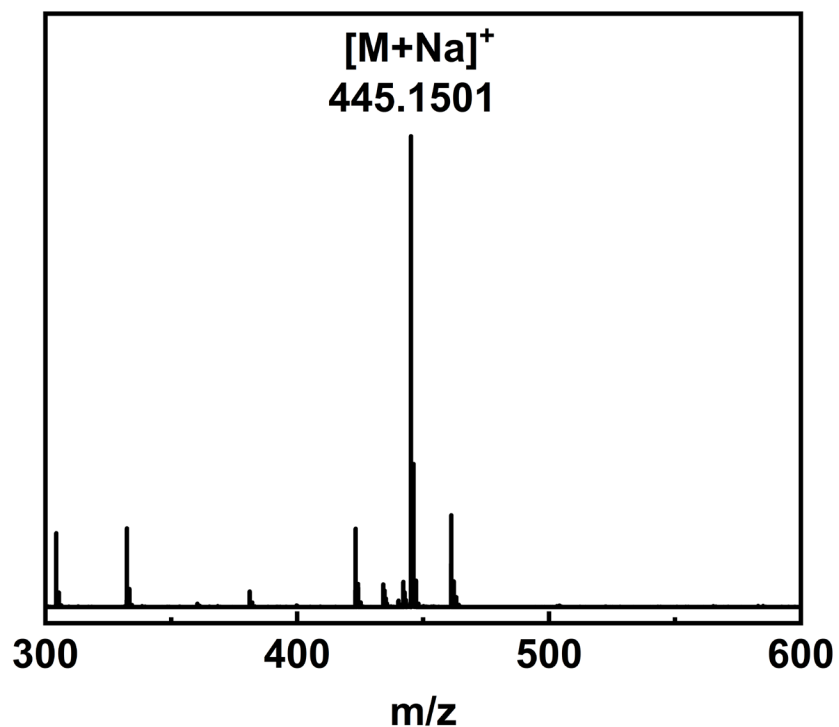


Fig. S3. ESI-TOF-MS of 4,4'bin-(acetyl)phenoxy-1,1'-biphenyl.

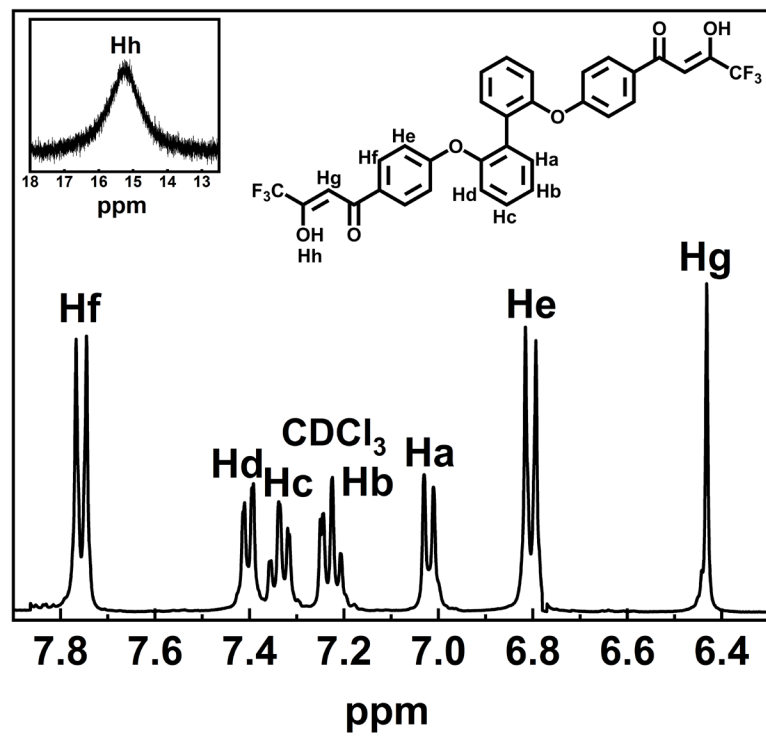


Fig. S4. 400 MHz ^1H NMR spectrum of L in CDCl_3 .

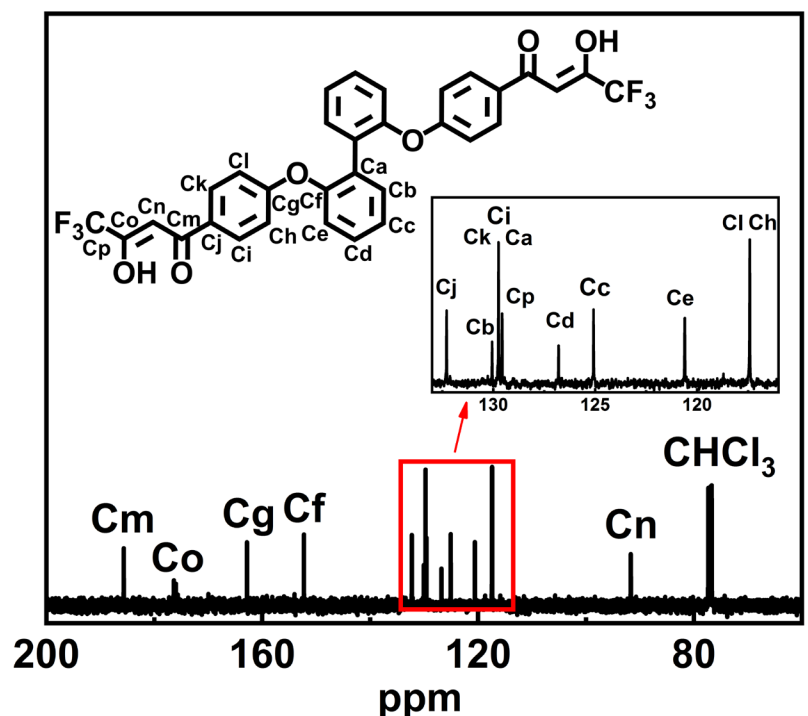


Fig. S5. 101 MHz ¹³C NMR spectrum of L in CDCl₃.

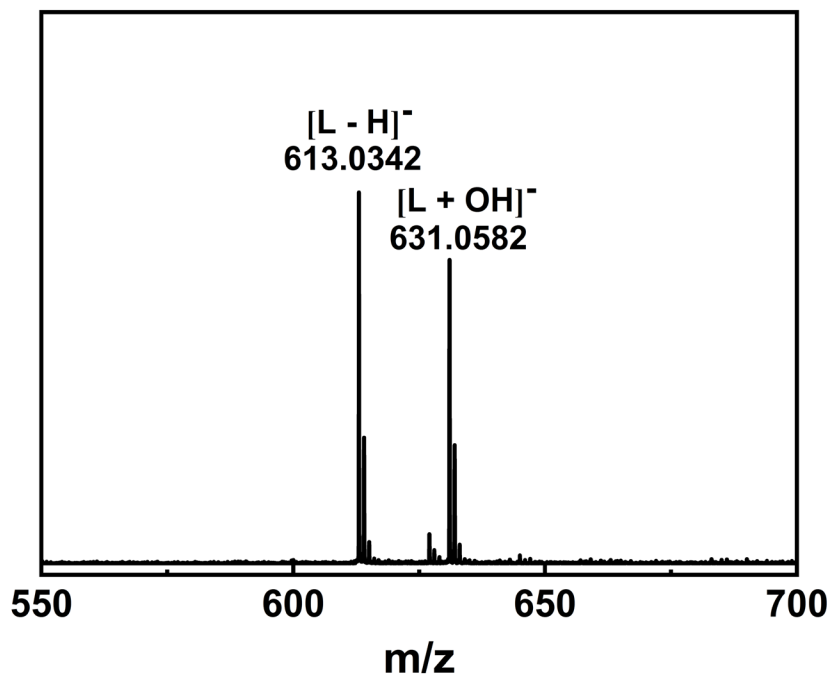


Fig. S6. ESI-TOF-MS of L.

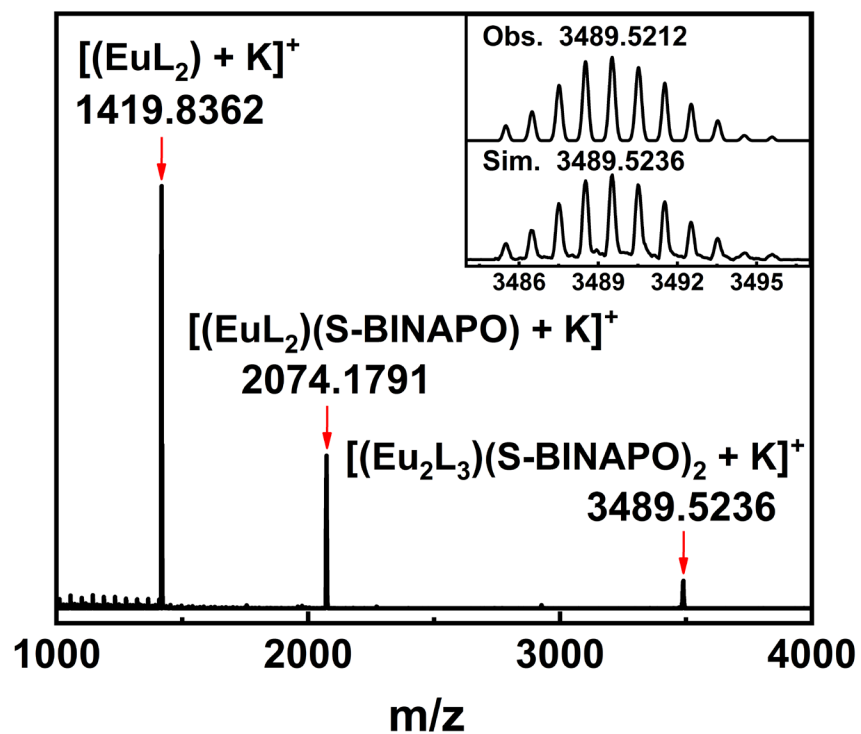


Fig. S7. ESI-TOF-MS of $(\text{Eu}_2\text{L}_3)(\text{S-BINAPO})_2$.

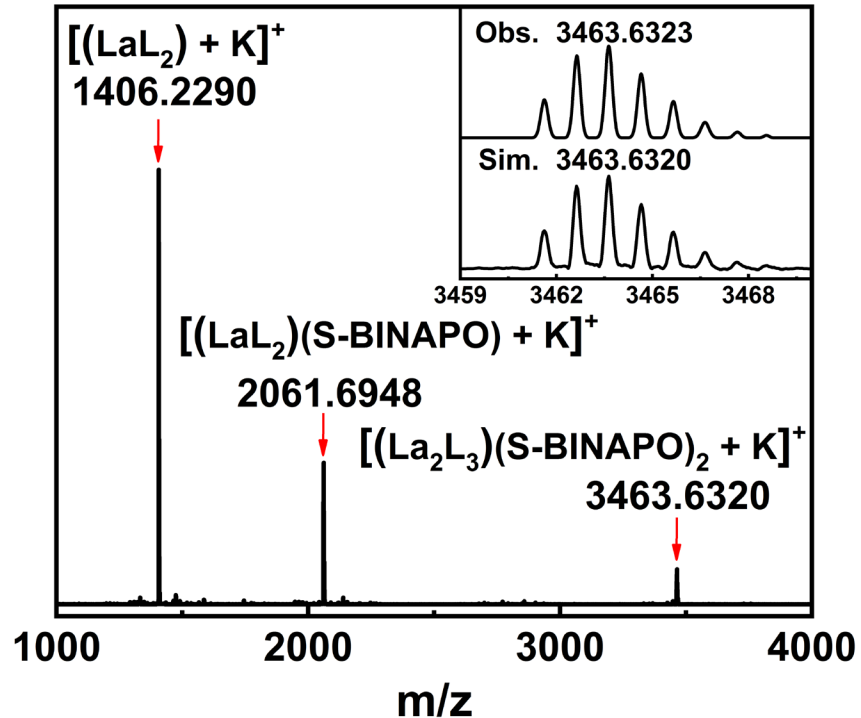


Fig. S8. ESI-TOF-MS of $(\text{La}_2\text{L}_3)(\text{R-BINAPO})_2$.

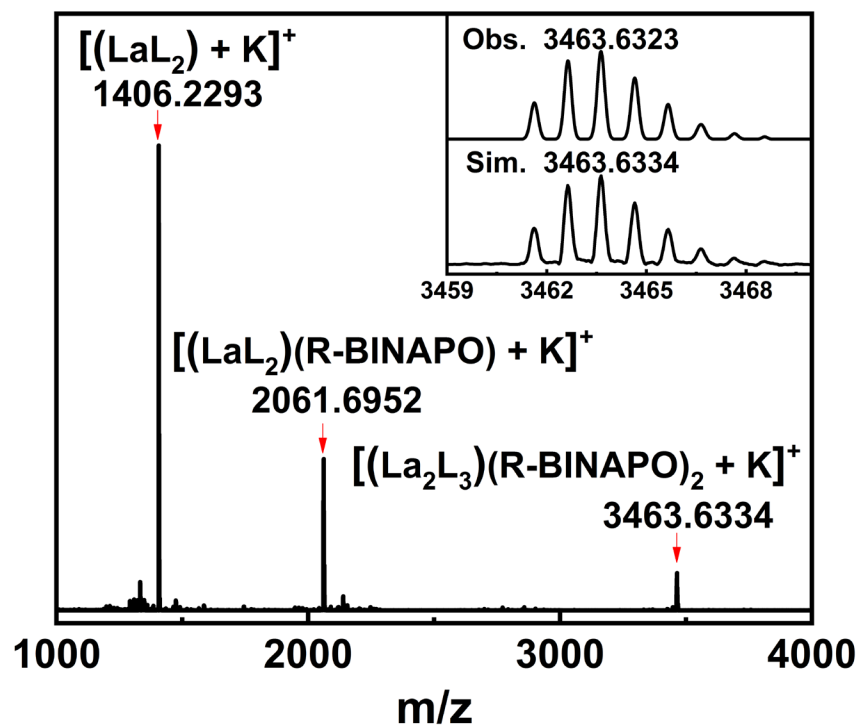


Fig. S9. ESI-TOF-MS of $(\text{La}_2\text{L}_3)(\text{S-BINAPO})_2$.

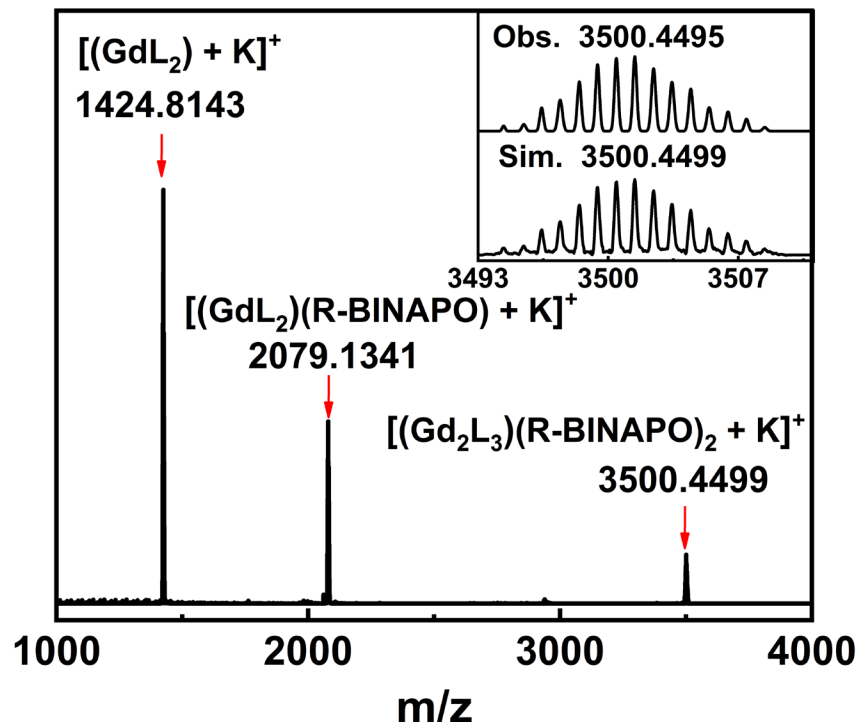


Fig. S10. ESI-TOF-MS of $(\text{Gd}_2\text{L}_3)(\text{R-BINAPO})_2$.

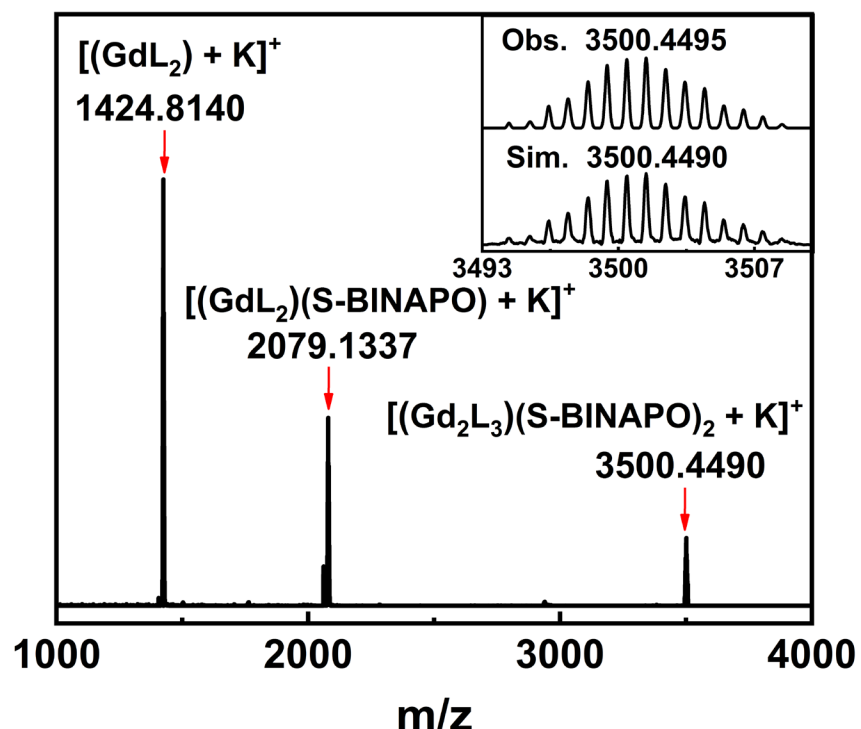


Fig. S11. ESI-TOF-MS of $(\text{Gd}_2\text{L}_3)(\text{S-BINAPO})_2$.

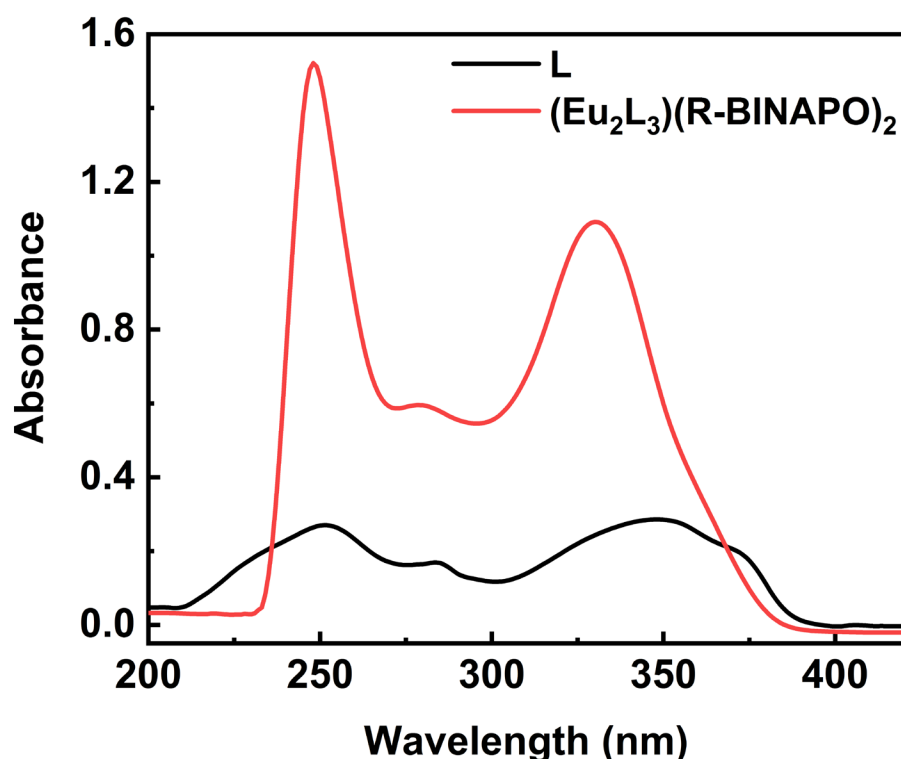


Fig. S12. UV-Vis absorption spectra of $(\text{Eu}_2\text{L}_3)(\text{R-BINAPO})_2$ (red line) (1.0×10^{-5} M), and L (black line) in $\text{CHCl}_3/\text{CH}_3\text{OH}$ (75:2) (1.0×10^{-5} M).

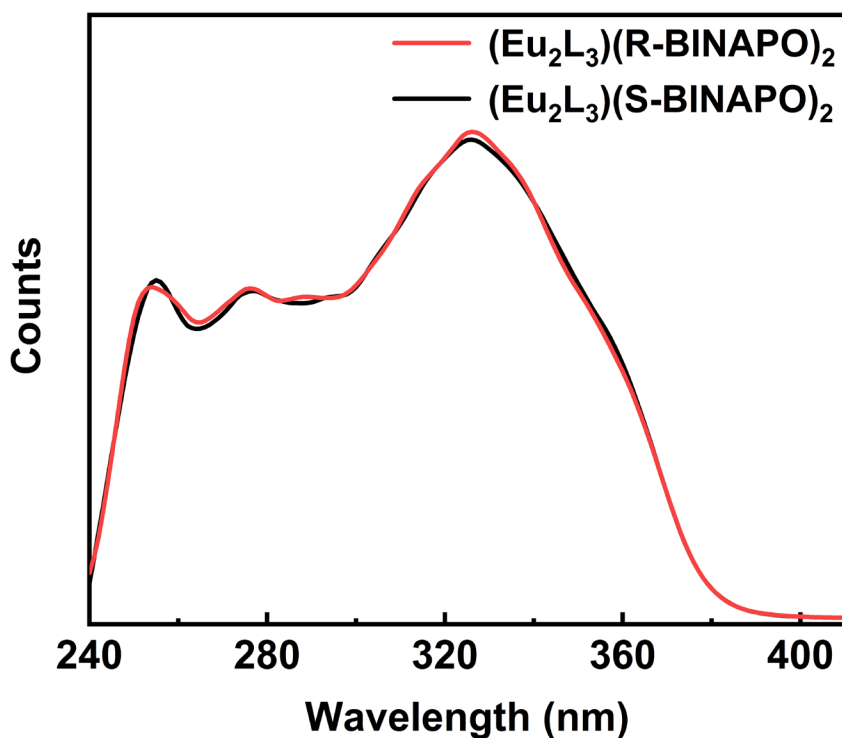


Fig. S13. Excitation spectra of $(\text{Eu}_2\text{L}_3)(\text{R-BINAPO})_2$ (red line) and $(\text{Eu}_2\text{L}_3)(\text{S-BINAPO})_2$ (black line) recorded by monitoring the emission band of Eu^{3+} ions at 612 nm in CHCl_3 (1×10^{-5} M).

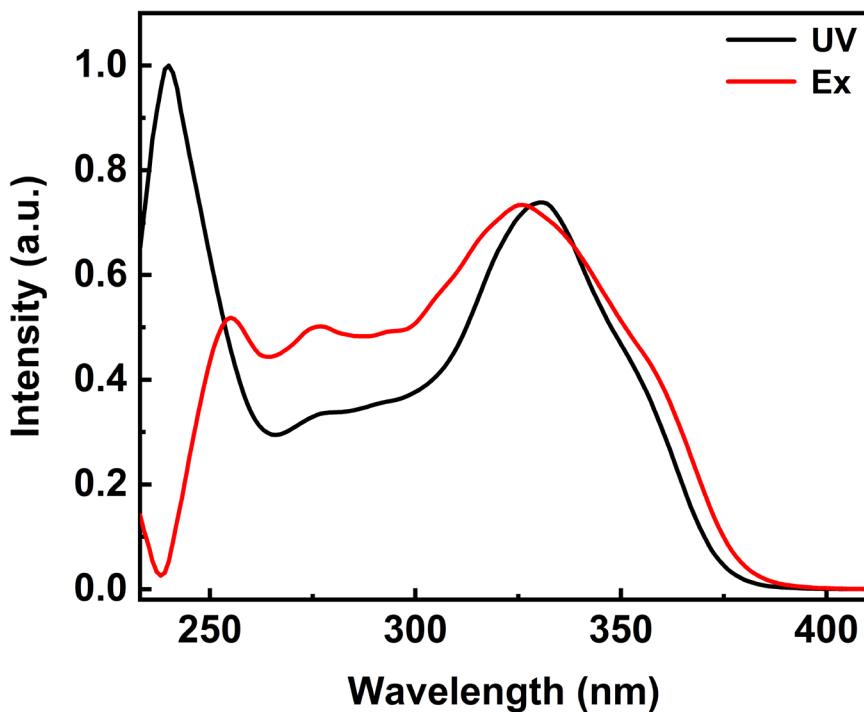


Fig. S14. Normalization absorption (black line) and excitation spectra (red line) of $(\text{Eu}_2\text{L}_3)(\text{R-BINAPO})_2$ in CHCl_3 .

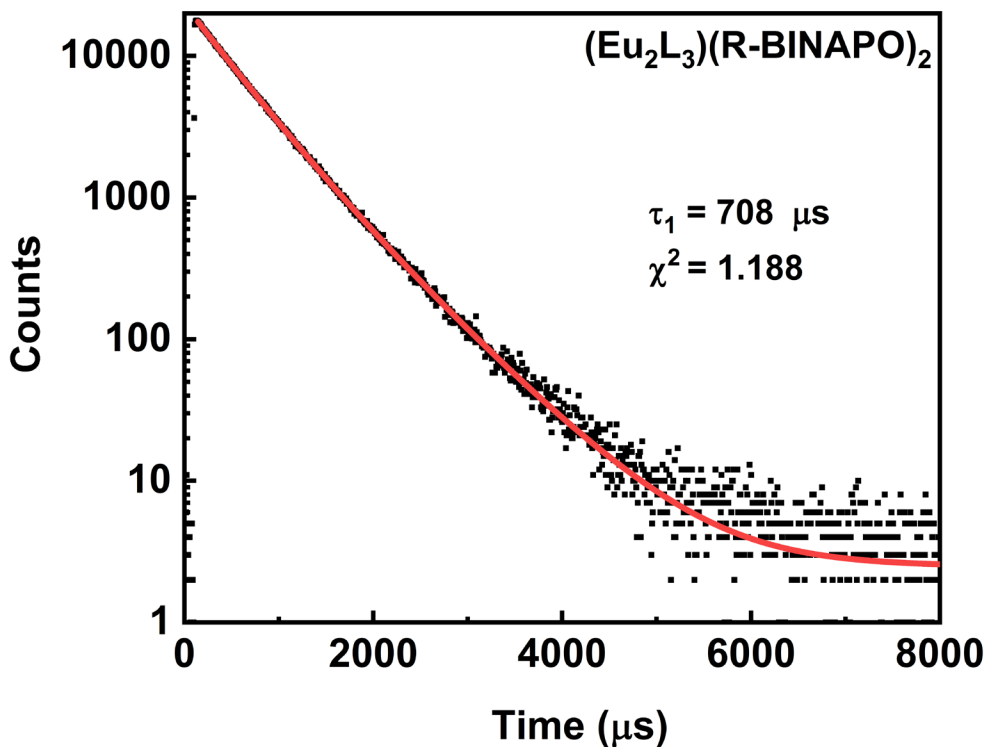


Fig. S15. Luminescence decay curve of $(\text{Eu}_2\text{L}_3)(\text{R-BINAPO})_2$ in CHCl_3 monitored at 612 nm.

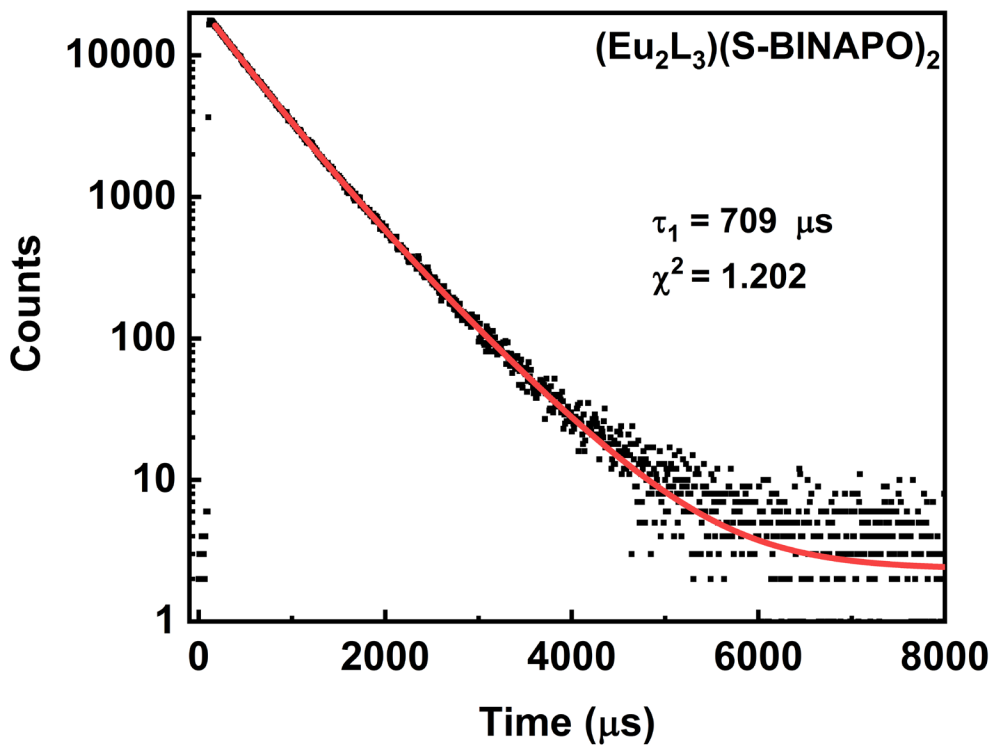


Fig S16. Luminescence decay curve of $(\text{Eu}_2\text{L}_3)(\text{S-BINAPO})_2$ in CHCl_3 monitored at 612 nm.

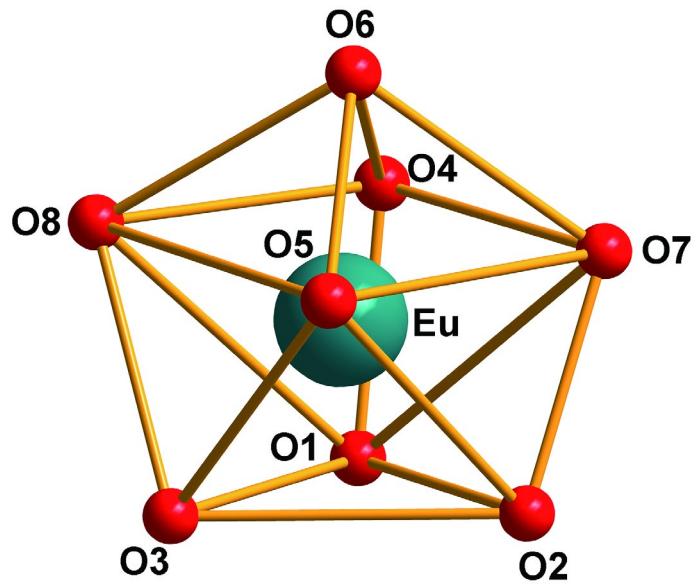


Fig. S17. Coordination polyhedra of $(\text{Eu}_2\text{L}_3)(\text{R-BINAPO})_2$.

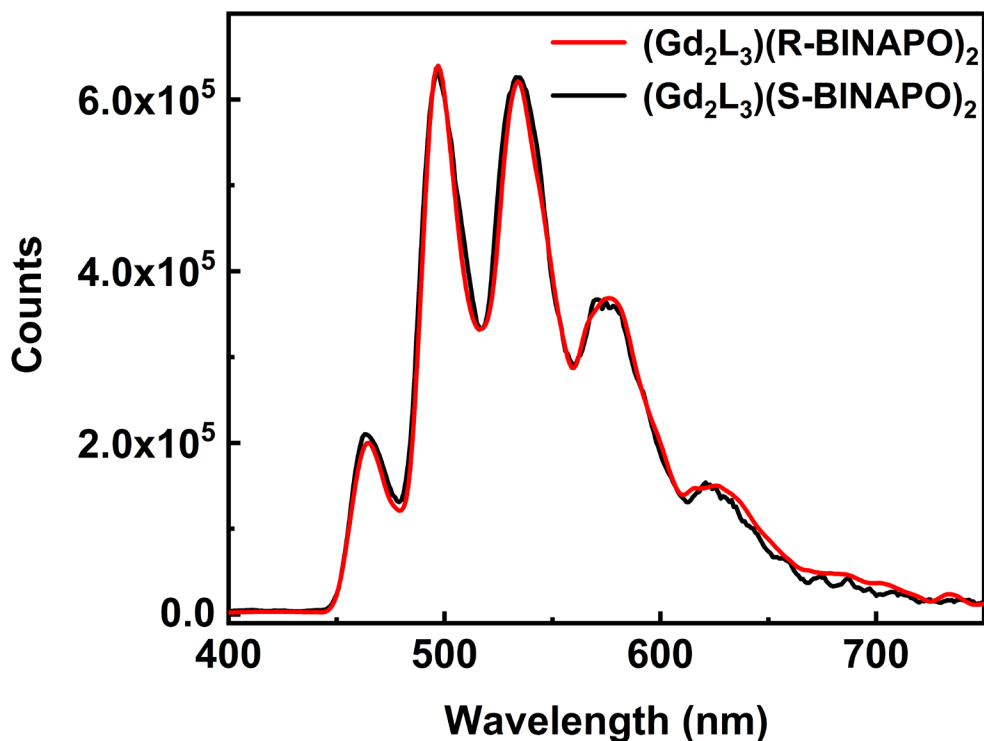


Fig. S18. Phosphorescence spectra of $(\text{Gd}_2\text{L}_3)(\text{R-BINAPO})_2$ (red line) and $(\text{Gd}_2\text{L}_3)(\text{S-BINAPO})_2$ (black line) in CHCl_3 at 77 K.